Hindawi Publishing Corporation
Mathematical Problems in Engineering
Volume 2015, Article ID 319054, 13 pages
http://dx.doi.org/10.1155/2015/319054

Research Article

The Solution of Two-Phase Inverse Stefan Problem Based on a Hybrid Method with Optimization

Yang Yu, Xiaochuan Luo, and Haijuan Cui

State Key Laboratory of Synthetical Automation for Process Industries, Northeastern University, Shenyang, Liaoning 110819, China

Correspondence should be addressed to Xiaochuan Luo; luoxch@mail.neu.edu.cn

Received 20 March 2015; Revised 30 April 2015; Accepted 4 May 2015

Academic Editor: Evangelos J. Sapountzakis

The two-phase Stefan problem is widely used in industrial field. This paper focuses on solving the two-phase inverse Stefan problem when the interface moving is unknown, which is more realistic from the practical point of view. With the help of optimization method, the paper presents a hybrid method which combines the homotopy perturbation method with the improved Adomian decomposition method to solve this problem. Simulation experiment demonstrates the validity of this method. Optimization method plays a very important role in this paper, so we propose a modified spectral DY conjugate gradient method. And the convergence of this method is given. Simulation experiment illustrates the effectiveness of this modified spectral DY conjugate gradient method.

1. Introduction

The process of solidification/melting occurs in many industrial fields, such as steel-making continuous casting. In the continuous casting process [1, 2], molten steel comes into slab by solidification. And this process is shown in Figure 1. Because of the heat symmetry, we only consider 1/2 of slab thickness, and we divide this domain into two regions by the freezing front, which is shown in Figure 2. D_1 stands for the solid phase and D_2 is taken by the liquid phase. The solidification problem of continuous casting is associated with Stefan problem, which is a model of the process with a phase change.

Many researches have focused on solving Stefan problems [3–7]. Grzymkowski and Slota [8, 9] applied the Adomian decomposition method (ADM) combined with optimization for solving the direct and the inverse one-phase Stefan problem, and Hetmaniok et al. [10] used the Adomian decomposition method (ADM) and variational iteration method to solve the one-phase Stefan moving boundary problems. In comparison to the studies on the one-phase Stefan problems, researches on two-phase Stefan problems [11] are much more scarce. Słota [12] applied homotopy perturbation method (HPM) to solve the two-phase inverse Stefan problem. However, in their formulation, these two-phase inverse Stefan problems were solved when the position of the moving interface is known. While the position of the moving interface is unknown and no temperature or heat flux boundary conditions are specified on one part of the boundary, this two-phase inverse Stefan problem may be difficult to be solved. This problem is close to the problem which occurs in the continuous casting. Therefore, this paper focuses on solving this problem by a hybrid method with optimization which combines the homotopy perturbation method (HPM) with the improved Adomian decomposition method (IADM).

This paper is organized as follows. In Section 2, we give the description of the two-phase Stefan problem. And the hybrid method for solving this problem is introduced in Section 3. We give a modified spectral DY conjugate gradient method and the convergence of this method in Section 4. In Section 5, some numerical results are given to illustrate the validity of the hybrid method.

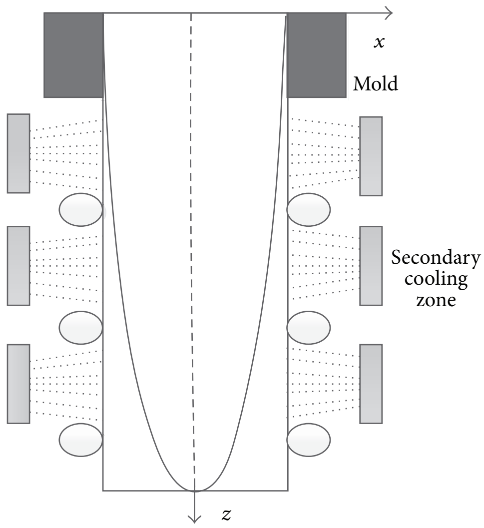

Figure 1: The solidification process of continuous casting slab (x stands for the direction of heat transfer and z stands for casting direction).

2. The Description of Two-Phase Inverse Stefan Problem

In this section, the two-phase inverse Stefan problem is considered. The two domains are described (see Figure 2):

$$D_1 = \{(x,t);\ x \in [0, \xi(t)],\ t \in [0, t^*]\},$$
$$D_2 = \{(x,t);\ x \in [\xi(t), d],\ t \in [0, t^*]\}, \tag{1}$$

and their boundaries with unknown function $x = \xi(t)$ are

$$\Gamma_1 = \{(x,0);\ x \in (0,s),\ s = \xi(0)\}, \tag{2}$$

$$\Gamma_2 = \{(x,0);\ x \in (s,d),\ s = \xi(0)\}, \tag{3}$$

$$\Gamma_3 = \{(0,t);\ t \in [0, t^*]\}, \tag{4}$$

$$\Gamma_4 = \{(d,t);\ t \in [0, t^*]\}, \tag{5}$$

$$\Gamma_5 = \{(x,t);\ t \in [0, t^*],\ x = \xi(t)\}, \tag{6}$$

$$\Gamma_6 = \{(x,t^*);\ x \in [0, \xi(t^*))\}. \tag{7}$$

In practice, the measurement of temperature on the boundary Γ_4 may not be easily obtained and the position of the moving interface described by means of function $x = \xi(t)$ is unknown. Therefore, the designed two-phase inverse Stefan problem consists in the calculation of the temperature distribution in the domains D_1 and D_2, respectively, as well as in the reconstruction of the functions describing moving interface $x = \xi(t)$. In order to solve this inverse problem, the additional information is given. In such a situation, the final time internal temperature at $t = t^*$ on the boundary Γ_6 is known, which can be measured in practice. The temperature distribution is determined by the functions $u_1(x,t)$ and $u_2(x,t)$, which are defined in the domains D_1 and D_2, respectively, and they satisfy the following heat conduction equations:

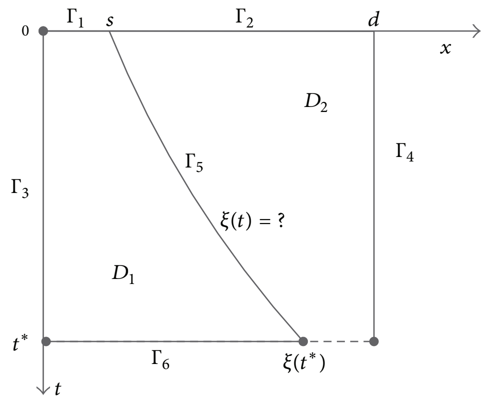

Figure 2: The domain formulation of the two-phase Stefan problem.

$$\frac{\partial u_1(x,t)}{\partial t} = \alpha_1 \frac{\partial^2 u_1(x,t)}{\partial x^2} \quad \text{in } D_1, \tag{8}$$

$$\frac{\partial u_2(x,t)}{\partial t} = \alpha_2 \frac{\partial^2 u_2(x,t)}{\partial x^2} \quad \text{in } D_2, \tag{9}$$

where t and x refer to time and spatial location and α_1 and α_2 are the thermal diffusivity in the solid phase and the liquid phase, respectively. On the boundaries Γ_1 and Γ_2, the initial conditions are described in the following:

$$u_1(x,0) = \varphi_1(x) \quad \text{on } \Gamma_1, \tag{10}$$

$$u_2(x,0) = \varphi_2(x) \quad \text{on } \Gamma_2, \tag{11}$$

$$\xi(0) = s. \tag{12}$$

On the boundary Γ_3, it satisfies the Dirichlet boundary or Neumann boundary condition:

$$u_1(0,t) = \theta_1(t) \quad \text{on } \Gamma_3. \tag{13}$$

On the boundary Γ_4, it satisfies the Dirichlet boundary conditions:

$$u_2(d,t) = \theta(t) \quad \text{on } \Gamma_4. \tag{14}$$

On the phase change moving interface (Γ_5), it satisfies the condition of temperature continuity and the Stefan condition:

$$u_1(\xi(t),t) = u_2(\xi(t),t) = u^*, \tag{15}$$

where u^* is the phase change temperature. Hence,

$$\kappa \frac{d\xi(t)}{t} = k_2 \left.\frac{\partial u_2(x,t)}{\partial x}\right|_{x=\xi(t)} - k_1 \left.\frac{\partial u_1(x,t)}{\partial x}\right|_{x=\xi(t)}, \tag{16}$$

where κ is the latent heat of fusion per unit volume and k_1 and k_2 are the thermal conductivity in the solid and liquid phase, respectively. The final time internal temperature on the boundary Γ_6 satisfies

$$u_1(x,t^*) = u_1^T(x) \quad \text{on } \Gamma_6. \tag{17}$$

3. The Solution of Two-Phase Inverse Stefan Problem

3.1. The Homotopy Perturbation Method. The homotopy perturbation method was presented in [13, 14]; it arose as a combination of two other methods: the perturbation method and the homotopy technique from topology. Homotopy perturbation method was applied on differential equations, partial differential equations, and the direct and inverse problems of heat transfer by many authors [15–17].

Homotopy perturbation method was used to find the exact or the approximate solutions of the linear and nonlinear integral equations [16, 18], the two-dimensional integral equations [19–21], and the integrodifferential equations [22–25]. This method enables seeking a solution of the following operator equation:

$$B(w)-\zeta(z)=0 \quad z\in\Omega, \tag{18}$$

where B is an operator, w is a sought function, and ζ is a known function on the domain of Ω. The operator B is presented in the form of sum:

$$B(v)=R(w)+Q(w), \tag{19}$$

where R defines the linear operator and Q is the remaining part of operator B. So (18) can be written as

$$R(w)+Q(w)-\zeta(z)=0 \quad z\in\Omega. \tag{20}$$

We define a new operator H which is called the homotopy operator in the following:

$$\begin{aligned} H(v,p)&=(1-p)\left(R(v)-R(w_0)\right)+p\left(B(v)-\zeta(z)\right)\\ &=0, \end{aligned} \tag{21}$$

where $p\in[0,1]$ is an embedding parameter, $v(z,p):\Omega\times[0,1]\to\mathfrak{R}$, and w_0 defines the initial approximation of a solution of (18); (21) is transformed into the following form:

$$\begin{aligned} H(v,p)=R(v)-R(w_0)+pR(w_0)&\\ +p\left(Q(v)-\zeta(z)\right)=0.& \end{aligned} \tag{22}$$

Therefore,

$$\begin{aligned} H(v,0)&=R(v)-R(w_0),\\ H(v,1)&=R(w_0)+Q(v)-\zeta(z). \end{aligned} \tag{23}$$

For $p=0$ the solution of operator equation $H(v,0)=0$ is equivalent to solution of problem $R(v)-R(w_0)=0$, whereas, for $p=1$, the solution of operator equation $H(v,1)=0$ is equivalent to solution of problem (20). Thus, a monotonous change of parameter p from zero to one is just that continuous change of the trivial problem $R(v)-R(w_0)=0$ to the original problem. In topology, this is called homotopy. According to the HPM, we assume that the solution of (21) and (22) can be written as a power series in p:

$$v=\sum_{i=0}^{\infty}p^i w_i=w_0+pw_1+p^2w_2+\cdots; \tag{24}$$

setting $p=1$, the approximate solution of (20) is obtained:

$$w=\lim_{p\to1}v=\sum_{i=0}^{\infty}w_i=w_0+w_1+w_2+\cdots; \tag{25}$$

in most cases, the series in (25) is convergent, and in [15] an additional remark on the convergence of this series can be found.

3.2. The Improved Adomian Decomposition Method. The Adomian decomposition method was presented by Adomian [26]. This method was used to solve a wide variety of linear and nonlinear problems. Several other researchers had developed a modification to the ADM [27]. The modification usually involves a slight change and it is aimed at improving the accuracy of the series solution.

The Adomian decomposition method is able to solve a wide class of nonlinear operator equations [28] in the form

$$F(u)=\eta, \tag{26}$$

where $F:H\to G$ is a nonlinear operator, η is a known element from Hilbert space G and u is the sought element from Hilbert space H. The operator $F(u)$ can be written as

$$F(u)=L(u)+R(u)+N(u), \tag{27}$$

where L is an invertible linear operator, R is a linear operator, and N is a nonlinear operator. The solution of (26) admits the decomposition into an infinite series of components

$$u=\sum_{i=0}^{\infty}g_i; \tag{28}$$

the nonlinear term N is equated to an infinite series

$$N(u)=\sum_{i=0}^{\infty}A_i; \tag{29}$$

A_n is the Adomian polynomials, which can be determined by

$$A_0=N(g_0), \tag{30}$$

$$A_n=\frac{1}{n!}\left[\frac{d^n}{d\lambda^n}N\left(\sum_{i=0}^{n}\lambda^i g_i\right)\right]_{\lambda=0} \quad n\geq1. \tag{31}$$

Substituting (28), (29), (30), and (31) into operator equation (26) and using the inverse operator L^{-1}, the following equation can be obtained:

$$\begin{aligned} g_0&=g^*+L^{-1}(\eta),\\ g_n&=-L^{-1}R(g_{n-1})-L^{-1}(A_{n-1}), \quad n\geq1, \end{aligned} \tag{32}$$

where g^* is the function dependent on the initial and boundary conditions.

The improved Adomian decomposition method [27]: it is important to note that the improved Adomian decomposition method is based on the assumption that the function

$y = g^* + L^{-1}(\eta)$ can be divided into two parts, namely, y_1 and y_2. Under this assumption, the following equation can be obtained:

$$y = y_1 + y_2. \tag{33}$$

Accordingly, a slight variation is proposed on the components g_0 and g_1. The suggestion is that only the part y_1 is assigned to the component g_0, whereas the remaining part y_2 is combined with other terms given in (33) to define g_1. Consequently, the recursive relation is written as follows:

$$\begin{aligned} g_0 &= y_1, \\ g_1 &= y_2 - L^{-1}R(g_0) - L^{-1}(A_0), \\ g_{n+2} &= -L^{-1}R(g_{n+1}) - L^{-1}(A_{n+1}) \quad n \geq 0. \end{aligned} \tag{34}$$

3.3. The Solution of the Two-Phase Inverse Stefan Problem. In this section, we introduce the solution of the two-phase inverse Stefan problem. We split the two-phase inverse Stefan problem into two problems. The first is the determination of $u_1(x,t)$ in domain D_1 and the moving interface $\xi(t)$ which is satisfying (7), (8), (10), and (13). Once the boundary $x = \xi(t)$ and the heat flux $(\partial u_2(x,t)/\partial x)|_{x=\xi(t)}$ have been obtained, the second problem for determining the temperature $u_2(x,t)$ in domain D_2 is solved.

The solution of $u_1(x,t)$ and moving interface $\xi(t)$ based on HPM: because the heat flux on the moving position is unknown in this two-phase inverse Stefan problem, the HPM is used to compute $u_1(x,t)$. In this section, the homotopy perturbation method is applied to solve the inverse problem. We make the homotopy map for (22):

$$H_1(v_1,p) = \frac{\partial^2 v_1}{\partial x^2} - \frac{\partial^2 u_{1,0}}{\partial x^2} + p\left(\frac{\partial^2 u_{1,0}}{\partial x^2} + \frac{1}{\alpha_1}\frac{\partial v_i}{\partial t}\right); \tag{35}$$

the solution to this equation,

$$H_1(v_1,p) = 0, \tag{36}$$

is sought in the form of a power series in p and it satisfies

$$v_1 = \sum_{i=0}^{\infty} p^i u_{1,i}, \tag{37}$$

where $p \in [0,1]$; by substituting (37) into (36), the following equation can be obtained:

$$\sum_{i=0}^{\infty} p^i \frac{\partial^2 u_{1,i}}{\partial x^2} = \frac{\partial^2 u_{1,0}}{\partial x^2} - p\frac{\partial^2 u_{1,0}}{\partial x^2} + \frac{1}{\alpha_1}\sum_{i=1}^{\infty}\frac{\partial u_{1,i-1}}{\partial t}. \tag{38}$$

Next, by comparing the same powers of parameter p in (38), the following equation can be obtained:

$$\frac{\partial^2 u_{1,1}}{\partial x^2} = \frac{1}{\alpha_1}\frac{\partial u_{1,0}}{\partial t} - \frac{\partial^2 u_{1,0}}{\partial x^2}, \tag{39}$$

$$\frac{\partial^2 u_{1,i}}{\partial x^2} = \frac{1}{\alpha_1}\frac{\partial u_{1,i-1}}{\partial t} \quad \text{for } i \geq 2. \tag{40}$$

Equations (39) and (40) must be supplemented by the boundary conditions. Therefore, for (39), we set the following boundary conditions:

$$u_{1,0}(0,t) + u_{1,1}(0,t) = \theta_1(t), \tag{41}$$

$$u_{1,0}(\xi(t),t) + u_{1,1}(\xi(t),t) = u^*, \tag{42}$$

and for (40) we set the conditions in the following ($i \geq 2$):

$$u_{1,i}(0,t) = 0, \tag{43}$$

$$u_{1,i}(\xi(t),t) = 0. \tag{44}$$

The above conditions are selected. So we give the n-order approximate solution:

$$\widehat{u}_{1,n} = \sum_{i=1}^{n} u_{1,i}, \tag{45}$$

because $u_{1,i}$ are determined by the unknown function $\xi(t)$. This function is derived in the form

$$\xi(t) = \sum_{i=1}^{m} c_i \psi_i(t). \tag{46}$$

Thus we define a cost function J_1 according to (10) and (17):

$$\begin{aligned} J_1(c_1,\ldots,c_m) = &\int_0^{\xi(0)} \{u_{1,n}(x,0) - \varphi_1(x)\}^2 dx \\ &+ \int_0^{\xi(t^*)} \{u_{1,n}(x,t^*) - u_1^T(x)\}^2 dx. \end{aligned} \tag{47}$$

Therefore, c_i are chosen according to the minimum of (47). The moving interface $\xi(t)$ and the solution of u_1 in domain D_1 can be obtained.

The boundary condition (13) on the boundary Γ_3 and the condition of temperature continuity (15) should be fulfilled for $n \geq 1$. In this way, while looking for the solution of this problem in domain D_1, the initial approximation $u_{1,1}$ will be found by solving the system of (39) with conditions (41) and (42). Conversely, functions $u_{1,i}, i = 1, 2, \ldots$, are determined by the recurrent solution of (40) with conditions (42) and (44). Consequently, the moving interface $\xi(t)$ and the solution of u_1 in domain D_1 can be obtained by the homotopy perturbation method with optimization. According to the Stefan condition (16) on the phase change moving interface Γ_5, the temperature $u_2(x,t)$ in domain D_2 can be recovered by IADM with optimization method.

The solution of $u_2(x,t)$ based on IADM with optimization: in this problem, we consider the operator equations (27), where

$$\begin{aligned} L(u_2) &= \frac{\partial^2 u_2}{\partial x^2}, \\ R(u_2) &= -\frac{1}{\alpha_2}\frac{\partial u_2}{\partial t}, \\ N(u_2) &= 0, \\ \eta &= 0. \end{aligned} \tag{48}$$

The inverse operator L^{-1} is given by the following equation:

$$L^{-1}(u_2) = \int_d^x \int_{\xi(t)}^x u_2(x,t)\,dx\,dx. \quad (49)$$

The boundary condition and the Stefan condition from (14) are used to obtain the following equation:

$$L^{-1}L\left(\frac{\partial^2 u_2}{\partial x^2}\right) = u_2(x,t) - \theta(t) - \left.\frac{\partial u_2(x,t)}{\partial x}\right|_{x=\xi(t)} (x-d). \quad (50)$$

Hence

$$g^* = \theta(t) + \left.\frac{\partial u_2(x,t)}{\partial x}\right|_{x=\xi(t)} (x-d); \quad (51)$$

then the following recursive relation can be obtained:

$$\begin{aligned} g_0 &= u_2(d,t) = \theta(t), \\ g_1 &= \left.\frac{\partial u_2(x,t)}{\partial x}\right|_{x=\xi(t)} (x-d) + \frac{1}{\alpha_2}\int_d^x \int_{\xi(t)}^x \frac{\partial g_0}{\partial t}\,dx\,dx, \\ g_{n+2} &= \frac{1}{\alpha_2}\int_d^x \int_{\xi(t)}^x \frac{\partial g_{n-1}}{\partial t}dx\,dx, \quad n \ge 0; \end{aligned} \quad (52)$$

because $u_1(x,t)$ and $\xi(t)$ are determined by the above HPM with optimization method, $(\partial u_2(x,t)/\partial x)|_{x=\xi(t)}$ can be obtained by (16). An approximation solution is expressed in the form

$$u_{2,n} = \sum_{i=0}^{n} g_i \quad n \in N, \quad (53)$$

and in this inverse Stefan problem, $\theta(t)$ is unknown on the boundary Γ_4 and it is derived in the following form:

$$\theta(t) = \sum_{i=1}^{m} q_i \phi_i(t), \quad (54)$$

where $q_i \in R$ and $\phi_i(t)$ are the basis function. The coefficients q_i are selected to show minimal deviation of function (55) from conditions (11) and (15). Thus q_i are chosen according to the minimum of the following functional:

$$J_2(q_1,\ldots,q_m) = \int_0^{t^*} \{u_{2,n}(\xi(t),t) - u^*\}^2\,dt + \int_{\xi(0)}^{d} \{u_{2,n}(x,0) - \varphi_2(x)\}^2\,dx, \quad (55)$$

where $J_2(q_1,\ldots,q_m)$ is a nonlinear function. The optimization method plays a very important role in solving this two-phase inverse Stefan problem. Therefore, a modified spectral DY conjugate gradient method is presented. In Section 4, this optimization method is introduced.

Remark. The IADM with optimization method can be used to solve the direct and inverse one-phase Stefan problem which is designed in the literature [8, 9]. And this method is better than ADM with optimization method. In Section 5, we give two examples of one-phase Stefan problem to illustrate the effectiveness of the IADM with optimization method.

4. A Modified Spectral DY Conjugate Gradient Method

Conjugate gradient methods are very efficient for solving the unconstrained optimization problem $\min_{x\in R_n} f(x)$. Their iterative formula is given as follows:

$$\begin{aligned} x_{k+1} &= x_k + \alpha_k d_k, \\ d_k &= \begin{cases} -g_k, & \text{if } k = 1; \\ -g_k + \beta_k d_{k-1} & \text{if } k \ge 1, \end{cases} \end{aligned} \quad (56)$$

where step-size α_k is positive, $g_k = \nabla f(x_k)$, and β_k is a scalar. In addition, α_k is a step length which is calculated by the line search. β_k is a very important factor in conjugate gradient methods; the FR, PRP, DY, and CD methods [29] are used for choosing this scalar. Among them, the DY method is regarded as one of the efficient conjugate gradient methods. The scalar β_k is given by

$$\beta_k^{\mathrm{DY}} = \frac{\|g_k\|}{d_{k-1}^T y_{k-1}}, \quad (57)$$

where $y_{k-1} = g_k - g_{k-1}$ and $\|\cdot\|$ stands for Euclidean norm. Recently, Birgin and Martłnez [30] presented a spectral conjugate gradient method which is combining conjugate gradient method and spectral gradient method. And the direction d_k is obtained by

$$\begin{aligned} d_k &= -\theta_k g_k + \beta_k d_{k-1}, \\ \beta_k &= \frac{(\theta_k y_{k-1} - s_{k-1})^T g_k}{d_{k-1}^T y_{k-1}}, \end{aligned} \quad (58)$$

where $\theta_k = s_{k-1}^T s_{k-1}/s_{k-1}^T y_{k-1}$ is a parameter with $s_{k-1} = x_k - x_{k-1}$ and θ_k is regarded as spectral gradient. However, according to [31], the spectral conjugate gradient method can not guarantee producing the descent directions.

Based on the above analysis, in the following, we describe a modified spectral DY conjugate gradient method and give the convergence of this method with the Wolfe type line search rules.

4.1. *The Modified Spectral DY Conjugate Gradient Method.*

The new method is introduced:

$$d_k = \begin{cases} -g_k, & \text{if } k = 1; \\ -\theta_k g_k + \beta_k d_{k-1} & \text{if } k \ge 1, \end{cases} \quad (59)$$

where $\theta_k = 1 + \|g_{k-1}\|^2/\|g_k\|^2$ and $\beta_k = \beta_k^{\mathrm{DY}}$. This method is called the MDY method.

Algorithm 1. Consider the following.

Step 1. The following are given: $x_0 \in R^n$, $\varepsilon > 0$, and the max iteration step $N_{\max}$.

Step 2. Set $k = 1$; compute $d_1 = -g_1 = -\nabla f(x_0)$; if $\|g_1\| \le \varepsilon$, then stop.

Step 3. Find α_k according to Wolfe type line search rule.

Step 4. Let $x_{k+1} = x_k + \alpha_k d_k$ and $g_{k+1} = g(x_{k+1})$; if $\|g_{k+1}\| \le \varepsilon$, then stop.

Step 5. Compute d_{k+1} by (59).

Step 6. Set $k = k + 1$; go to Step 3.

4.2. Convergence Analysis. From the above, the MDY conjugate gradient method provides a descent direction for the objective function. In the following, we give the convergence of this algorithm with the Wolfe type line search rules. Firstly, we introduce some assumptions:

(i) The level set $\Omega = \{x \in R^n \mid f(x) \le f(x_1)\}$ is bounded.

(ii) In some neighborhood N of Ω, $f(x)$ is continuously differentiable and its gradient is Lipschitz continuous; namely, there exists a constant $L > 0$ such that

$$\|g(x) - g(y)\| \le L\|x - y\|, \quad \forall x, y \in N. \tag{60}$$

It is implied from the above assumptions that there exist two positive constants β and γ such that

$$\begin{gathered} \|x\| \le B, \\ \|g(x)\| \le \gamma, \\ \forall x \in \Omega. \end{gathered} \tag{61}$$

The Wolfe type line search [29] is

$$f(x_k) - f(x_k + \alpha_k d_k) \ge \delta\alpha_k^2 \|d_k\|^2, \tag{62}$$

$$g(x_k + \alpha_k d_k)^T d_k \ge -2\delta\alpha_k \|d_k\|^2, \tag{63}$$

and the strong Wolfe line search is

$$f(x_k + \alpha_k d_k) \le f(x_k) + \delta\alpha_k g_k^T d_k, \tag{64}$$

$$\left|g(x_k + \alpha_k d_k)^T d_k\right| \le \left|\sigma g_k^T d_k\right|, \tag{65}$$

where $0 < \delta < \sigma < 1$.

Lemma 2. *Let the sequences $\{g_k\}$ and $\{d_k\}$ be generated by the proposed algorithm (Algorithm 1) with Wolfe type line search rules; then $g_k^T d_k < 0$ and*

$$\beta_k^{\mathrm{DY}} \le \frac{g_k^T d_k}{g_{k-1}^T d_{k-1}}. \tag{66}$$

Proof. According to (59), we have

$$\begin{aligned} g_k^T d_k &= -\theta_k \|g_k\|^2 + \beta_k^{\mathrm{DY}} g_k^T d_{k-1} \\ &= \beta_k^{\mathrm{DY}} \left[-\theta_k d_{k-1}\left(g_k^T - g_{k-1}^T\right) + g_k^T d_{k-1}\right] \\ &= \beta_k^{\mathrm{DY}} \left[g_{k-1}^T d_{k-1} - \frac{\|g_{k-1}\|^2 d_{k-1} y_{k-1}^T}{\|g_k\|^2}\right] \\ &\le \beta_k^{\mathrm{DY}} g_{k-1}^T d_{k-1}. \end{aligned} \tag{67}$$

If we choose $k = 1$, then

$$g_1^T d_1 = -\|g_1\|^2 < 0; \tag{68}$$

according to (65), we have

$$y_1^T d_1 \ge (\sigma - 1) g_1^T d_1 \ge 0. \tag{69}$$

So $\beta_2^{\mathrm{DY}} \ge 0$. For $k > 1$, according to (67), we have

$$g_k^T d_k < 0, \tag{70}$$

by induction. So we obtain

$$\beta_k^{\mathrm{DY}} \le \frac{g_k^T d_k}{g_{k-1}^T d_{k-1}}; \tag{71}$$

the proof is completed. □

Theorem 3. *Let the sequences $\{g_k\}$ and $\{d_k\}$ be generated by the proposed algorithm (Algorithm 1) with Wolfe type line search rules; then*

$$g_k^T d_k \le -\overline{C} \parallel g_k\|^2, \tag{72}$$

where $\overline{C} > 0$ is a constant.

Proof. According to (59), we have

$$\begin{aligned} g_k^T d_k &= -\theta_k \|g_k\|^2 + \beta_k^{\mathrm{DY}} g_k^T d_{k-1} \\ &= -\|g_{k-1}\|^2 + \left(\frac{g_k^T d_{k-1}}{d_{k-1}^T y_{k-1}} - 1\right)\|g_k\|^2 \\ &\le \left(\frac{g_{k-1}^T d_{k-1}}{d_{k-1}^T y_{k-1}}\right)\|g_k\|^2. \end{aligned} \tag{73}$$

From the Wolfe type line search rules (65), we can obtain

$$-(\sigma + 1) g_{k-1}^T d_{k-1} \ge d_{k-1}^T (g_k - g_{k-1}) > 0; \tag{74}$$

according to (73) and (74), we have

$$g_k^T d_k \le -\frac{1}{\sigma + 1}\|g_k\|^2; \tag{75}$$

we define $\overline{C} = 1/(\sigma + 1)$. Therefore, we can obtain inequality (72). □

Lemma 4. *Suppose that assumptions (i) and (ii) hold; let $\{g_k\}$ and $\{d_k\}$ be generated by the proposed algorithm (Algorithm 1) with Wolfe type line search rules (62) and (63); then one has*

$$\sum_{k\geq 0}\frac{\left(g_k^T d_k\right)^2}{\|d_k\|^2}\leq\infty. \tag{76}$$

Proof. From assumption (ii), we have

$$\left\|g\left(x_k+\alpha_k d_k\right)^T-g\left(x_k\right)^T\right\|\leq L\left\|\alpha_k d_k\right\|, \tag{77}$$

so we can obtain

$$\left\|g\left(x_k+\alpha_k d_k\right)^T d_k-g\left(x_k\right)^T d_k\right\|\leq L\alpha_k\left\|d_k\right\|^2. \tag{78}$$

From inequality (63), we obtain

$$2\sigma\alpha_k\left\|d_k\right\|^2\geq -g\left(x_k+\alpha_k d_k\right)^T d_k. \tag{79}$$

According to inequalities (78) and (79), we have

$$(2\sigma+L)\,\alpha_k\left\|d_k\right\|^2\geq -g_k^T d_k. \tag{80}$$

So we can obtain

$$\alpha_k\left\|d_k\right\|\geq\frac{1}{2\sigma+L}\left(\frac{-g_k^T d_k}{\|d_k\|}\right). \tag{81}$$

Owing to inequality (81), we have

$$\begin{aligned}\sum_{k=1}^{\infty}\left(\frac{-g_k^T d_k}{\|d_k\|}\right)&\leq(2\sigma+L)^2\sum_{k=1}^{\infty}\alpha_k^2\left\|d_k\right\|^2\\&\leq(2\sigma+L)^2\sum_{k=1}^{\infty}\left\{f\left(x_k\right)-f\left(x_{k+1}\right)\right\}\\&<+\infty.\end{aligned} \tag{82}$$

From (82), we can obtain inequality (76). □

Theorem 5. *Suppose that assumptions (i) and (ii) hold. Let $\{g_k\}$ and $\{d_k\}$ be generated by the algorithm with Wolfe type line search rules. Then one has*

$$\liminf_{k\to\infty}\left\|g_k\right\|=0. \tag{83}$$

Proof. By contradiction, we suppose that there exists a positive constant $\overline{\gamma}>0$, such that

$$\left\|g_k\right\|\geq\overline{\gamma} \tag{84}$$

holds for all $k>1$. From (59), we have

$$\left\|d_k\right\|^2=-2\theta_k d_k^T g_k+\left(\beta_k^{\mathrm{DY}}\right)^2\left\|d_{k-1}\right\|^2-\theta_k^2\left\|g_k\right\|^2. \tag{85}$$

According to Lemma 4 and the above equation, we have

$$\left\|d_k\right\|^2\leq\left(\frac{g_k^T d_k}{g_{k-1}^T d_{k-1}}\right)^2\left\|d_{k-1}\right\|^2-\theta_k^2\left\|g_k\right\|^2-2\theta_k d_k^T g_k. \tag{86}$$

Multiplying the above inequality by $1/(g_k^T d_k)^2$, we have

$$\begin{aligned}\frac{\|d_k\|^2}{\left(g_k^T d_k\right)^2}&\leq\frac{\|d_{k-1}\|^2}{\left(g_{k-1}^T d_{k-1}\right)^2}-\left(\frac{\theta_k\|g_k\|}{g_k^T d_k}+\frac{1}{\|g_k\|}\right)^2\\&\quad+\frac{1}{\|g_k\|^2}\leq\frac{\|d_{k-1}\|^2}{\left(g_{k-1}^T d_{k-1}\right)^2}+\frac{1}{\|g_k\|^2}\\&\leq\sum_{i=1}^{k}\frac{1}{\left\|g_i^2\right\|^2}\leq\frac{1}{\overline{\gamma}^2}k.\end{aligned} \tag{87}$$

Then from inequality (83), we have

$$\sum_{k=1}^{\infty}\frac{\left(g_k^T d_k\right)^2}{\|g_k\|^2}\geq\overline{\gamma}^2\sum_{k=1}^{\infty}\frac{1}{k}=\infty, \tag{88}$$

which contradicts (76). Therefore, (83) holds. □

5. Numerical Simulation Experiments

In order to illustrate the validity of the IADM with optimization method, we introduce the one-phase inverse Stefan problem in Example 1. From the literature [9], we know the inverse Stefan problem consists in the calculation of the temperature distribution in the domain and in the reconstruction of the temperature distribution on the boundary, when the position of the function which describes the moving interface is known. And then, in Example 2, we solve the two-phase inverse Stefan problem based on the hybrid method which combines the Adomian decomposition method with the homotopy perturbation method.

Example 1. In this example, the one-phase inverse Stefan problem [9] is taken for the following values of parameters: $\alpha_1=1$, $k_1=1$, $u^*=1$, $t^*=1/2$, $\kappa=1/\alpha_1$, $\varphi_1(x)=\exp(\alpha_1 x)$, and $u_1^T(x)=\exp(\alpha_1/2-x)$. Then the exact solution of such formulated one-phase Stefan problem can be found from the following functions:

$$\begin{aligned}u_1(x,t)&=\exp\left(\alpha_1 t-x\right),\\\theta_1(t)&=\exp\left(\alpha_1 t\right),\\\xi(t)&=\alpha_1 t.\end{aligned} \tag{89}$$

The following equation,

$$\phi_i(t)=\exp\left(-(i-1)\,t\right)\quad i=1,2,\ldots,m, \tag{90}$$

is taken as basis function. The approximate solutions are compared with the exact solution and the values of the absolute errors are calculated from

$$\begin{aligned}\delta_h&=\left\{\int_0^{t^*}\left[h_e(t)-h_r(t)\right]dt\right\}^{1/2},\\\delta_u&=\left\{\int\int_D\left[u_e(x,t)-u_n(x,t)\right]dx\,dt\right\}^{1/2},\end{aligned} \tag{91}$$

where $h(t) \in \{\theta(t), \xi(t)\}$ ($\theta(t)$ stands for the boundary condition on Γ_1 in the literature [9] and $\xi(t)$ is the moving interface), D is the domain of the temperature distribution, $h_e(t)$ is the exact value of function $h(t)$, $h_r(t)$ is the approximate value of function $h(t)$, $u_e(x,t)$ is the exact distribution of the temperature in the domain, and $u_n(x,t)$ is the reconstructed distribution of temperature. Percentage relative errors are calculated from

$$\Delta_h = \frac{\delta_h}{\sqrt{\int_0^{t^*} [h_e(t)]^2 \, dt}} \times 100\%,$$
$$\Delta_u = \frac{\delta_u}{\sqrt{\int \int_D [u_e(x,t)]^2 \, dx \, dt}} \times 100\%. \quad (92)$$

The comparison of the ADM and the IADM for reconstructing distribution of the temperature on boundary Γ_1 in the literature [9] is shown in Figure 3 for $n = 1$, $n = 2$ and $m = 2$, $m = 3$. From Figure 3, the method based on the improved Adomian decomposition method (IADM) is better than the Adomian decomposition method (ADM).

Example 2. This example is introduced to illustrate the effectiveness of the hybrid method which combines the Adomian decomposition method with the homotopy perturbation method, which is presented in the previous sections. Here, we consider an example of the two-phase inverse Stefan problem [12], in which $\alpha_1 = 5/2$, $\alpha_2 = 5/4$, $k_1 = 6$, $k_2 = 2$, $\kappa = 4/5$, $u^* = 1$, $t^* = 1$, $d = 3$, $s = 3/2$, and $\varphi_1(x) = e^{(3-2x)/10}$, $\varphi_2(x) = e^{(3-2x)/5}$, $\theta_1(t) = e^{(t+3)/10}$, and $u_1^T(x) = e^{(4-2x)/10}$. The exact solution of this inverse Stefan problem is described by the following functions:

$$u_1(x,t) = e^{(t-2x+3)/10},$$
$$u_2(x,t) = e^{(t-2x+3)/5},$$
$$\theta(t) = e^{(t-3)/5}, \quad (93)$$
$$\xi(t) = \frac{(t+3)}{2}.$$

First, we use HPM with optimization method to solve $u_1(x,t)$ and $\xi(t)$. As the initial approximation $u_{1,0}$, this fulfills the initial condition:

$$u_{1,0}(x,t) = e^{(3-2x)/10}. \quad (94)$$

By using the function $u_{1,0}$ in (39) and the conditions (41) and (42), the following system of equations can be obtained:

$$\frac{\partial^2 u_{1,1}(x,t)}{\partial x^2} = -\frac{1}{25} e^{(3-2x)/10}. \quad (95)$$

With the conditions

$$u_{1,1}(0,t) = e^{3/10}\left(e^{(t/10)-1}\right),$$
$$u_{1,1}(x,t)\big|_{x=\xi(t)} = 1 - e^{(3-2\xi(t))/10}, \quad (96)$$

this system of equations can be solved. And the solution of this system is shown in the following:

$$u_{1,1}(x,t) = -e^{3/10-x/5} + \frac{1-e^{(3+t)/10}}{\xi(t)} x + e^{(t+3)/10}. \quad (97)$$

Next, we designate the functions $u_{1,i}$ for $i \geq 2$ in the following:

$$\frac{\partial^2 u_{1,i}}{\partial x^2} = \frac{2}{5}\frac{\partial u_{1,i-1}}{\partial t}, \quad (98)$$

and the conditions are shown:

$$u_{1,i}(0,t) = 0,$$
$$u_{1,i}(x,t)\big|_{x=\xi(t)} = 0. \quad (99)$$

By using (98) and the boundary conditions (99), we derive $u_{1,i}(x,t)$ for $i \geq 2$; according to (45), the approximate solution $u_1(x,t)$ is obtained. Here, we define basis functions according to (46):

$$\psi_i(t) = t^{i-1} \quad i = 1, \ldots, m. \quad (100)$$

We use the modified spectral DY (MDY) conjugate gradient method to solve function (47). The solution of moving interface $\xi(t)$ is shown in Figure 4. So the temperature $u_1(x,t)$ is derived in domain D_1. Values of the error in reconstruction of the position of the moving interface $\xi(t)$ and the temperature distribution $u_1(x,t)$ are shown in Table 1.

In order to verify the validity of the modified spectral DY (MDY) conjugate gradient method, we choose $n = 2$, $m = 2$, $\varepsilon = 10^{-4}$, the initial point $c_0 = (2.2, 2.5)$, and the max step number $N_{\max} = 100$. The comparison results of DY and MDY are shown in Figure 5 and Table 2. Comparing to DY conjugate gradient method, the MDY conjugate gradient method is slightly better.

The moving interface $\xi(t)$ and $u_1(x,t)$ in domain D_1 are obtained by the homotopy perturbation method with optimization. Next, with the help of condition (16), we can determine the temperature $u_2(x,t)$ in domain D_2 by the improved Adomian decomposition method (IADM) with optimization. Without loss of generality, we choose the basis functions

$$\phi_i(t) = t^{i-1}, \quad i = 1, \ldots, m. \quad (101)$$

The exact and the reconstructed distribution of the temperature on boundary Γ_4 are shown in Figure 6 for different number of basis functions $\phi_i(t)$. And the errors in reconstruction of the temperature $\theta(t)$ (on boundary Γ_4 in Figure 2) and the temperature distribution $u_2(x,t)$ are shown in Table 3. The inversion results of the function $\theta(t)$ match the exact value very well.

The measured temperature $u_1^T(x)$ at the final time t^* on the boundary Γ_6 in Figure 2 is perturbed by the random error. So in the next section we consider the influence of measurement errors on the results. We set the measured

Table 1: Values of the error in reconstruction of the position of the moving interface and the temperature distribution $u_1(x,t)$.

HPM	δ_ξ	Δ_ξ	δ_{u_1}	Δ_{u_1}
$n=2, m=2$	0.108712413045	0.61599738364	0.116978666115	0.109525848228
$n=2, m=3$	0.210642147214	1.19356205914	0.299360015653	0.280470260729
$n=2, m=3$	0.015061910569	0.08534533677	0.102526697222	0.096057215386

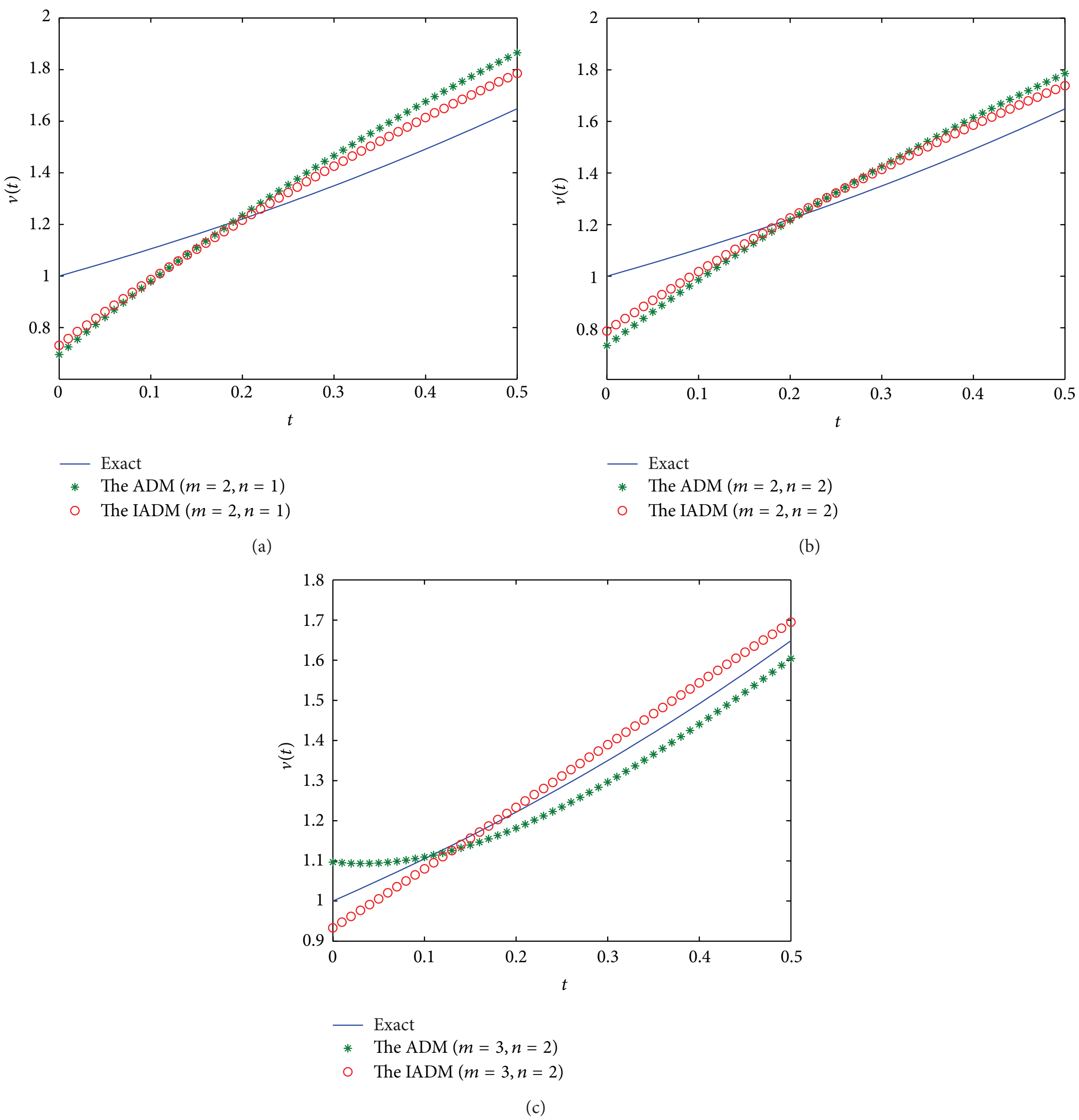

Figure 3: The reconstructing distribution of the temperature on boundary (Γ_1 in the literature [9]) for $n=1$, $n=2$ and $m=2$, $m=3$.

temperature $u_1^T(x)$ with an error of 1% and 3%. We can obtain the moving interface $\xi(t)$ and $\theta(t)$; the results are shown in Figures 7 and 8.

In Figures 7 and 8, the exact and the reconstructed distribution of the temperature on moving interface $\xi(t)$ and the boundary Γ_4 are shown, and the errors in reconstruction of the function describing the moving interface and boundary conditions are compiled in Table 4. The obtained reconstruction results illustrate that the functions $\xi(t)$ and $\theta(t)$ are reconstructed very well. From the results, the hybrid

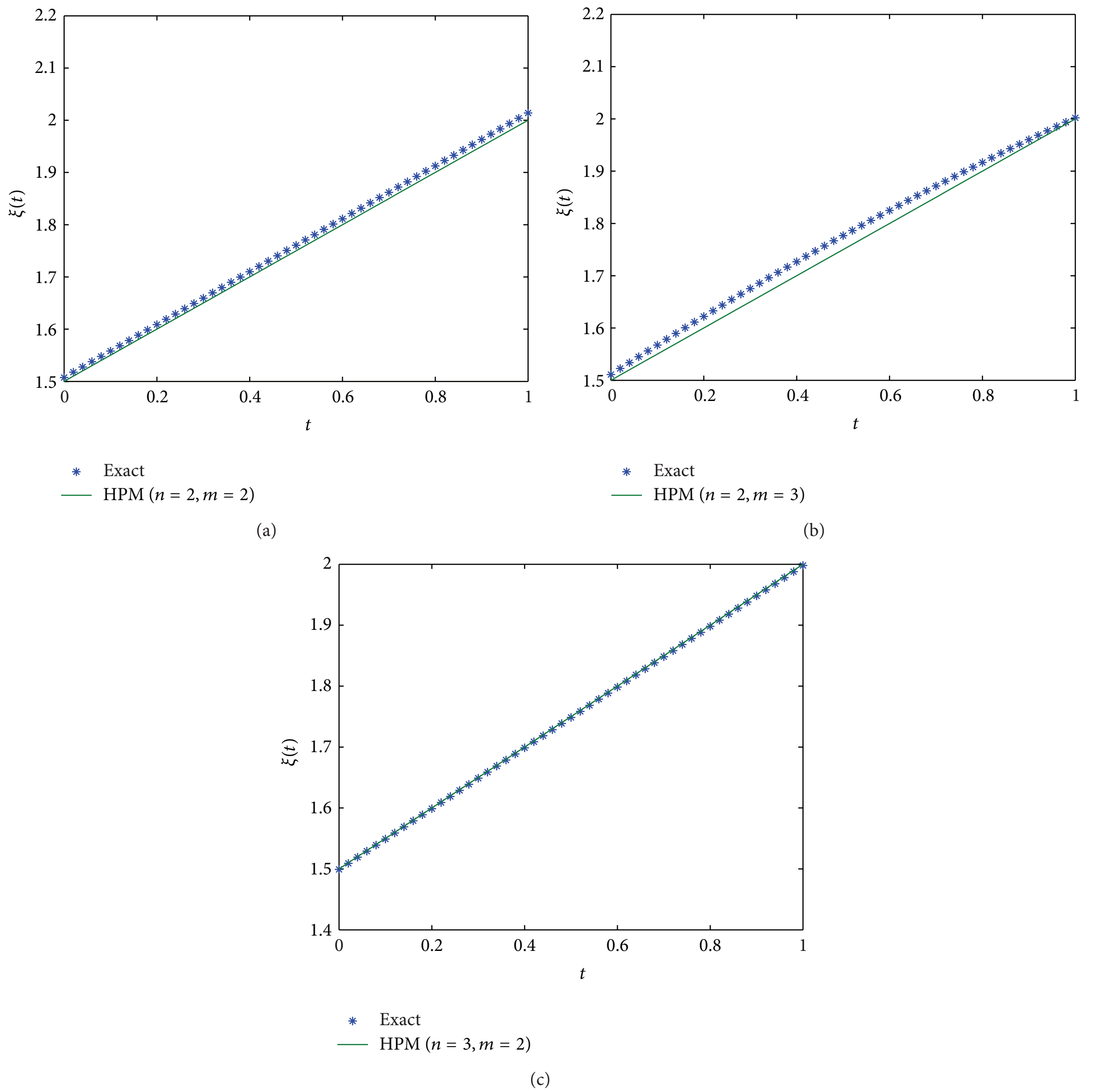

Figure 4: The position of moving interface $\xi(t)$.

Table 2: The comparison results of DY and MDY.

Algorithm	Iteration numbers	Optimization value
DY	50	$(1.52, 0.48)$
MDY	23	$(1.51, 0.501)$

method with optimization is stable with the input errors. When the input data are contaminated by the errors, the error of the reconstructed boundary conditions does not exceed the error of the input data.

6. Conclusion

Based on the homotopy perturbation method (HPM) with the improved Adomian decomposition method (IADM), a hybrid method with optimization is proposed to solve the two-phase inverse Stefan problem. This problem is more realistic from the practical point of view. The simulation experiment is used to verify this method. Experimental results match the exact value very well. Furthermore, this investigated method can also be used for solving one-phase direct Stefan problems.

Optimization method is very crucial in this paper, so a modified spectral DY conjugate gradient method is

TABLE 3: Values of the error in reconstruction of the temperature $\theta(t)$ on boundary Γ_4 in Figure 2 and the temperature distribution $u_2(x,t)$.

IADM	$\delta_{\theta(t)}$	$\Delta_{\theta(t)}$	$\delta_{u_2(x,t)}$	$\Delta_{u_2(x,t)}$
$n = 2, m = 2$	0.0125536846	0.20525000280	0.649823007	0.5444948151
$n = 2, m = 3$	0.00907338187	0.14834781217	0.717820233	0.6014705398

TABLE 4: Values of the error in reconstruction the moving interface $\xi(t)$ and the temperature $\theta(t)$ on boundary Γ_4 in Figure 2.

Perturbation error on the $u_1^T(x)$	$\delta_{\xi(t)}$	$\Delta_{\xi(t)}$	$\delta_{\theta(t)}$	$\Delta_{\theta(t)}$
1% error	0.0968150593	0.771949532	0.032490326	0.7475026727
3% error	0.3725894970	2.9708217908	0.061914613	1.4244652005

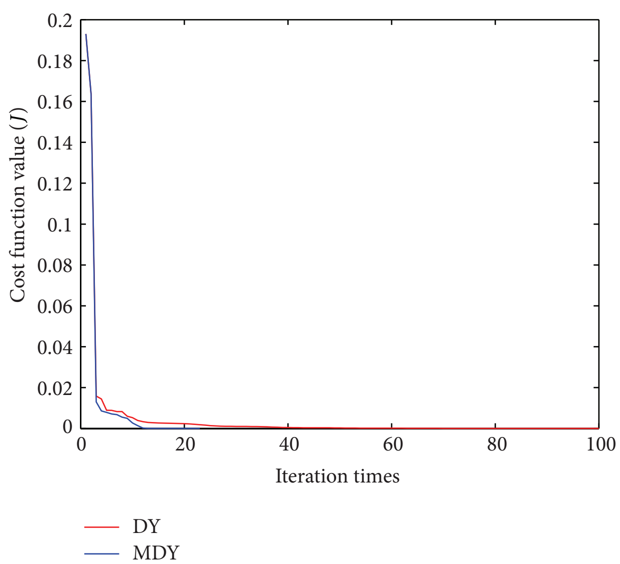

FIGURE 5: The cost function J_1 changes with the increasing of iteration numbers.

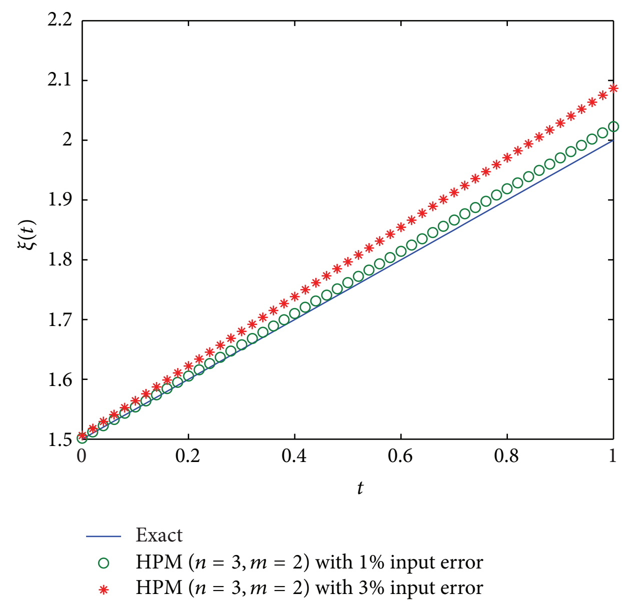

FIGURE 7: The reconstructed position of moving interface $\xi(t)$.

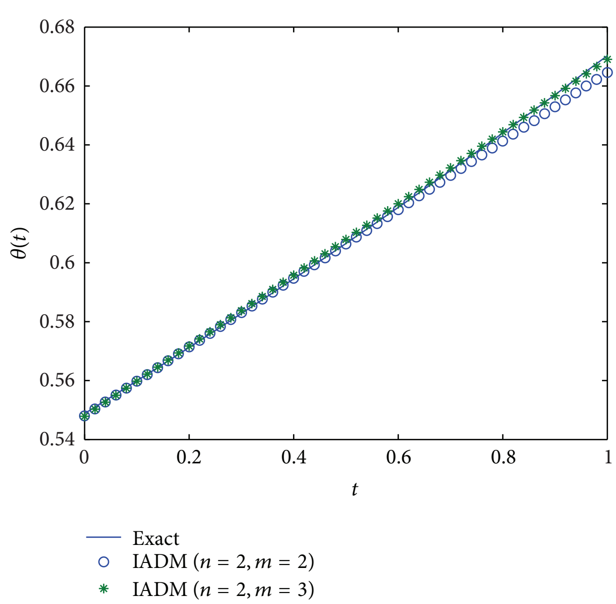

FIGURE 6: The reconstructing distribution of the temperature $\theta(t)$ on boundary Γ_4 in Figure 2.

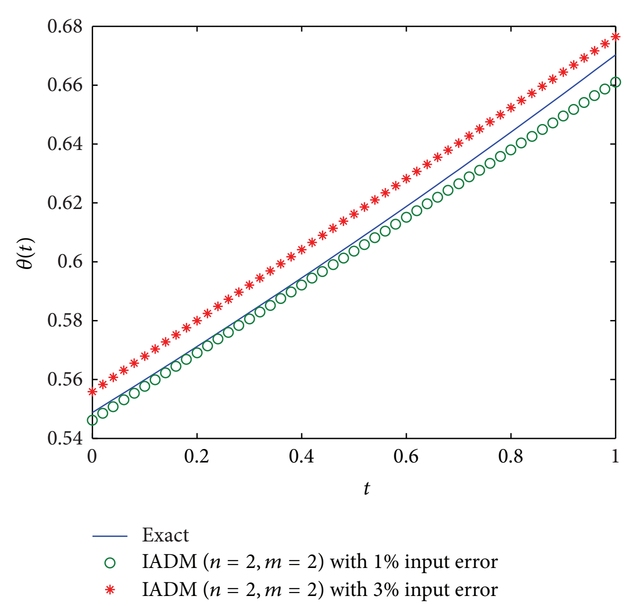

FIGURE 8: The reconstructing distribution of the temperature $\theta(t)$ on boundary Γ_4 in Figure 2.

presented. And we give the convergence of this MDY method. Simulation experiment illustrates the validity of this optimization method.

Conflict of Interests

The authors declare that there is no conflict of interests regarding the publication of this paper.

Acknowledgments

This work was supported by the National Natural Science Foundation of China (60974091, 61333006, and 61473074) and the Fundamental Research Funds for the Central Universities (N120708001).

References

[1] A. Fic, A. J. Nowak, and R. Bialecki, "Heat transfer analysis of the continuous casting process by the front tracking BEM," *Engineering Analysis with Boundary Elements*, vol. 24, no. 3, pp. 215–223, 2000.

[2] C. A. Santos, J. A. Spim, and A. Garcia, "Mathematical modeling and optimization strategies (genetic algorithm and knowledge base) applied to the continuous casting of steel," *Engineering Applications of Artificial Intelligence*, vol. 16, no. 5-6, pp. 511–527, 2003.

[3] R. Kamal, A. Hojatollah, A. R. Jamal, and P. Kourosh, "Application of mesh-free methods for solving the inverse one dimensional Stefan problem," *Engineering Analysis with Boundary Elements*, vol. 40, pp. 1–21, 2014.

[4] D. Slota, "Direct and inverse one-phase Stefan problem solved by the variational iteration method," *Computers & Mathematics with Applications*, vol. 54, no. 7-8, pp. 1139–1146, 2007.

[5] B. T. Johansson, D. Lesnic, and T. Reeve, "A method of fundamental solutions for the one-dimensional inverse Stefan problem," *Applied Mathematical Modelling. Simulation and Computation for Engineering and Environmental Systems*, vol. 35, no. 9, pp. 4367–4378, 2011.

[6] D. Slota, "The application of the homotopy perturbation method to one-phase inverse Stefan problem," *International Communications in Heat and Mass Transfer*, vol. 37, no. 6, pp. 587–592, 2010.

[7] R. Grzymkowski, M. Pleszczyński, and D. Slota, "Comparing the Adomian decomposition method and the Runge-Kutta method for solutions of the Stefan problem," *International Journal of Computer Mathematics*, vol. 83, no. 4, pp. 409–417, 2006.

[8] R. Grzymkowski and D. Slota, "Stefan problem solved by Adomian decomposition method," *International Journal of Computer Mathematics*, vol. 82, no. 7, pp. 851–856, 2005.

[9] R. Grzymkowski and D. Slota, "One-phase inverse Stefan problem solved by adomian decomposition method," *Computers & Mathematics with Applications*, vol. 51, no. 1, pp. 33–40, 2006.

[10] E. Hetmaniok, D. Słota, R. Wituła, and A. Zielonka, "Comparison of the Adomian decomposition method and the variational iteration method in solving the moving boundary problem," *Computers & Mathematics with Applications*, vol. 61, no. 8, pp. 1931–1934, 2011.

[11] B. T. Johansson, D. Lesnic, and T. Reeve, "A meshless method for an inverse two-phase one-dimensional linear Stefan problem," *Inverse Problems in Science and Engineering*, vol. 21, no. 1, pp. 17–33, 2013.

[12] D. Słota, "Homotopy perturbation method for solving the two-phase inverse stefan problem," *Numerical Heat Transfer Part A: Applications*, vol. 59, no. 10, pp. 755–768, 2011.

[13] J. H. He, "Homotopy perturbation technique," *Computer Methods in Applied Mechanics and Engineering*, vol. 178, no. 3-4, pp. 257–262, 1999.

[14] J.-H. He, "An elementary introduction to the homotopy perturbation method," *Computers & Mathematics with Applications*, vol. 57, no. 3, pp. 410–412, 2009.

[15] C. Chun, H. Jafari, and Y.-I. Kim, "Numerical method for the wave and nonlinear diffusion equations with the homotopy perturbation method," *Computers & Mathematics with Applications*, vol. 57, no. 7, pp. 1226–1231, 2009.

[16] A. Yildirim, "Analytical approach to fractional partial differential equations in fluid mechanics by means of the homotopy perturbation method," *International Journal of Numerical Methods for Heat & Fluid Flow*, vol. 20, no. 2, pp. 186–200, 2010.

[17] E. Hetmaniok, I. Nowak, D. Slota, R. Witula, and A. Zielonka, "Solution of the inverse heat conduction problem with neumann boundary condition by using the homotopy perturbation method," *Thermal Science*, vol. 17, no. 3, pp. 643–650, 2013.

[18] J. Biazar and H. Ghazvini, "Numerical solution for special nonlinear Fredholm integral equation by HPM," *Applied Mathematics and Computation*, vol. 195, no. 2, pp. 681–687, 2008.

[19] X. Zhang, J. Zhao, J. Liu, and B. Tang, "Homotopy perturbation method for two dimensional time-fractional wave equation," *Applied Mathematical Modelling*, vol. 38, no. 23, pp. 5545–5552, 2014.

[20] M. Ghasemi, M. Tavassoli Kajani, and E. Babolian, "Application of He's homotopy perturbation method to nonlinear integro-differential equations," *Applied Mathematics and Computation*, vol. 188, no. 1, pp. 538–548, 2007.

[21] A. Golbabai and M. Javidi, "Application of He's homotopy perturbation method for n th-order integro-differential equations," *Applied Mathematics and Computation*, vol. 190, no. 2, pp. 1409–1416, 2007.

[22] J. Biazar, Z. Ayati, and M. R. Yaghouti, "Homotopy perturbation method for homogeneous Smoluchowski's equation," *Numerical Methods for Partial Differential Equations*, vol. 26, no. 5, pp. 1146–1153, 2010.

[23] A. Alawneh, K. Al-Khaled, and M. Al-Towaiq, "Reliable algorithms for solving integro-differential equations with applications," *International Journal of Computer Mathematics*, vol. 87, no. 7, pp. 1538–1554, 2010.

[24] H. Aminikhah and J. Biazar, "A new analytical method for solving systems of Volterra integral equations," *International Journal of Computer Mathematics*, vol. 87, no. 5, pp. 1142–1157, 2010.

[25] J. Biazar, B. Ghanbari, M. G. Porshokouhi, and M. G. Porshokouhi, "He's homotopy perturbation method: a strongly promising method for solving non-linear systems of the mixed Volterra-Fredholm integral equations," *Computers & Mathematics with Applications*, vol. 61, no. 4, pp. 1016–1023, 2011.

[26] G. Adomian, *Stochastic Systems*, vol. 169 of *Mathematics in Science and Engineering*, Academic Press, New York, NY, USA, 1983.

[27] M. Almazmumy, F. A. Hendi, H. O. Bakodah, and H. Alzumi, "Recent modifications of Adomian decomposition method for initial value problem in ordinary differential equations,"

American Journal of Computational Mathematics, vol. 2, no. 3, pp. 228–234, 2012.

[28] D. Lesnic, "Convergence of Adomian's decomposition method: periodic temperatures," *Computers & Mathematics with Applications*, vol. 44, no. 1-2, pp. 13–24, 2002.

[29] W. Cao, K. R. Wang, and Y. L. Wang, "Global convergence of a modified spectral CD conjugate gradient method," *Journal of Mathematical Research & Exposition*, vol. 31, pp. 261–268, 2011.

[30] E. G. Birgin and J. M. Martłnez, "A spectral conjugate gradient method for unconstrained optimization," *Applied Mathematics and Optimization*, vol. 43, no. 2, pp. 117–128, 2001.

[31] L. Zhang, W. J. Zhou, and D. H. Li, "Global convergence of a modified Fletcher-Reeves conjugate gradient method with Armijo-type line search," *Numerische Mathematik*, vol. 104, no. 4, pp. 561–572, 2006.


Advances in Operations Research
Advances in Decision Sciences
Journal of Applied Mathematics
Algebra
Journal of Probability and Statistics
The Scientific World Journal
Hindawi
Submit your manuscripts at
http://www.hindawi.com
International Journal of Differential Equations
International Journal of Combinatorics
Advances in Mathematical Physics
Journal of Complex Analysis
Journal of Mathematics
Mathematical Problems in Engineering
Abstract and Applied Analysis
Discrete Dynamics in Nature and Society
International Journal of Mathematics and Mathematical Sciences
Journal of Discrete Mathematics
Journal of Function Spaces
International Journal of Stochastic Analysis
Journal of Optimization